

## **DISCLAIMER**

**This report was prepared as an account of work sponsored by an agency of the United States Government. Neither the United States Government nor any agency Thereof, nor any of their employees, makes any warranty, express or implied, or assumes any legal liability or responsibility for the accuracy, completeness, or usefulness of any information, apparatus, product, or process disclosed, or represents that its use would not infringe privately owned rights. Reference herein to any specific commercial product, process, or service by trade name, trademark, manufacturer, or otherwise does not necessarily constitute or imply its endorsement, recommendation, or favoring by the United States Government or any agency thereof. The views and opinions of authors expressed herein do not necessarily state or reflect those of the United States Government or any agency thereof.**

## **DISCLAIMER**

**Portions of this document may be illegible in electronic image products. Images are produced from the best available original document.**

DOE/CE/34012-1

To: Dana Dixon  
Department of Energy  
Chicago Operations Office  
9800 S. Cass Ave.  
Argonne, IL 60439  
June 20, 2003

DOE Patent Clearance Granted  
*M. Dvorscak* 7.16.03  
Date  
Mark P. Dvorscak  
(630) 252-2393  
E-mail: mark.dvorscak@ch.doe.gov  
Office of Intellectual Property Law  
DOE Chicago Operations Office

Final Report for Grant # DE-FG02-87CE34012  
For the Period of 6/87/-5/01  
Total Value of Grant \$150,000  
Prepared by: Erin K. Goodwin, Assistant Director of Meetings and Exhibits

During the period in question, the money received under grant # DE-FG02-87CE34012 was expended in the following way:

1987- Supported the summer fellowships for the following five students (Names unavailable)

1988- Supported the summer fellowships for the following five students (Names unavailable)

1989 Supported the summer fellowships for the following five students (Names unavailable)

1990- Supported the summer fellowships for the following five student: C. K. Nguyen, I.-H. Oh, T. G. Strein, J. W. Weidner, S. E. Gilbert

1991- Supported the summer fellowships for the following five student: C. S. Johnson H. Huang, D. R. Lawson, B. D. Pendley, C. C. Streinz

1992- Supported the summer fellowships for the following five students: P. A. Connick, A. C. Miller, D. L. Taylor, K. K. Lian, T. T. Nadasdi

1993- Supported the summer fellowships for the following five students: D. G. Jensen, J. C. Bart, G. Seshandri, J. A. Poirier, K. W. Vogt

1994- Supported the summer fellowships for the following five students: Z. Shi, C.-C. Hsueh, V. A. Adamian, K. M. Maness, K. M. Richard

1995- Supported the summer fellowships for the following five students: Y.-E. Sung, J. C. Conboy, L. A. Zook, W. R. Everett, H. Zhang

1996- Supported the summer fellowships for the following five students: S. Motupally, J.-B. D. Greenl, S. Nayak, C. Nasr, S. Y. Grabtchak

1997- Supported the summer fellowships for the following five students: C. Horne, K. Hu, K. Jennings, M.E. Williams, A. Zolfaghari

1998- Supported the summer fellowships for the following five students: M. Elhamid, J. Ritchie, S. Sriramulu, M. Zhao, S. Zou

1999- Supported the summer fellowships for the following five students: S.S. Wong, D. Gall, G. Hasselmann, D. Hooks, and S. Minter

2000- Supported the summer fellowships for the following five students: K. Cooper, K. Grant, D. Hansen, J.F. Hicks, Z. Liu

Sincerely,

Erin K. Goodwin  
Assistant Director of Meetings and Exhibits

**Final Report for DE-FG02-96ER 25289**

*Simpson*  
*1001535*  
*Math*  
*Robin*

The following papers were produced under this contract:

1. (With D. Owen), Antiplane Shear Flows in Visco-Plastic Solids Exhibiting Isotropic and Kinematic Hardening, SIAM J. of Appl. Math, 58, 6, 1996-2023 (1998).
2. (With R. C. MacCamy and C. V. Coffman), On the Long-time Behavior of Ferroelectric Systems, CMU Center for Nonlinear Analysis Research Report No. 97-NA-011, September 1997, Physica D 134, 362-383 (1999).
3. Estimates and Computations for Melting and Solidification Problems, CMU Center for Nonlinear Analysis Research Report No. 99-CNA-019, September 1999 and Mathematical Modelling and Numerical Analysis Vol. 35, No. 4. 607-630 (2001).
4. Melt Fracture Revisited, CMU Center for Nonlinear Analysis Research Report No. 00-CNA-004, April 2000 and EJAM Vol. 12, 465-477 (2001).
5. Extensions and Amplifications of a Traffic Model of Aw and Rascle. CMU Center for Nonlinear Analysis Research Report No. 00-CNA-010, August 2000. and SIAM J. Appl. Math. Vol. 62, No. 3, 729-745 (2001).
6. A Rigorous Treatment of a Follow-the-Leader Traffic Model with Traffic Lights Present (with B. Argall, E. Cheleshkin, C. Hinde, P-J Lin), CMU Center for Nonlinear Analysis Research Report No. 01-CNA-007, May 2001 and to appear in SIAM J. Appl. Math.
7. Congestion on Multilane Highways (with A. Klar, M. Rascle), CMU Center for Nonlinear Analysis Research Report No. 01-CNA-011, September 2001, to appear in SIAM J. Appl. Math.
8. Phase Transitions with Semi-Diffuse Interfaces, CMU Center for Nonlinear Analysis Research Report No. 01-CNA-014, October 2001 and to appear in J. Diff. Eqs.

One student, Andrew Yershov was supported on the contract. He completed his degree December 18, 1998. His thesis title was, "Numerical Methods for the Shallow Water Equations."

# Congestion on Multilane Highways

July 1, 2002

J. M. Greenberg<sup>1</sup>

A. Klar<sup>2</sup>

M. Rascle<sup>3</sup>

## Abstract

We present a new model for traffic on a multilane freeway (with  $n$  lanes). Our basic descriptors are the car density  $\rho$  (in cars/mile) taken across all lanes in the freeway and the average car velocity  $u$  (in miles/hour). The flux of cars across all lanes is given by  $\rho u = \sum_{i=1}^n \rho_i u_i$  where  $\rho_i$  is the car density in the  $i^{\text{th}}$  lane and  $u_i$  the velocity of cars in the  $i^{\text{th}}$  lane. We shall only track  $\rho$  and  $u$  and not what is going on in each individual lane.

On such multilane freeways one often observes distinct stable equilibrium relationships between auto velocity and density. Prototypical situations involve two equilibria

$$v = v_1(\rho) > v = v_2(\rho) \quad , \quad 0 \leq \rho < \rho_{\max}$$

where  $v_1(\cdot)$  and  $v_2(\cdot)$  are monotone decreasing and satisfy  $v_1(\rho_{\max}) = v_2(\rho_{\max}) = 0$ . The upper curve is typically stable for densities satisfying  $0 \leq \rho \leq \rho_1$  whereas the lower curve is stable for densities satisfying  $\rho_2 \leq \rho \leq \rho_{\max}$ . Our interest is in the situation where  $0 < \rho_2 \leq \rho_1 < \rho_{\max}$  and  $v_2(\rho_2) \leq v_1(\rho_1)$ .

In this paper we present a model which incorporates both equilibrium curves and a simple switching mechanism which allows cars to transit from one equilibrium curve to the other. This switching mechanism, when combined with the continuity equation, produces relaxation or self-excited oscillations in the system and these oscillations are what interests us here.

## 1 Introduction

In this paper we present a new model for traffic on a multilane freeway with  $n$  lanes. Our basic descriptors are the car density  $\rho$  (in cars/mile) taken across all lanes in the freeway and the average car velocity  $u$  (in miles/hour). The flux of cars across all lanes is given by  $\rho u = \sum_{i=1}^n \rho_i u_i$  where  $\rho_i$  is the car density in the  $i^{\text{th}}$  lane and  $u_i$  the velocity of cars in the  $i^{\text{th}}$  lane. We shall only track  $\rho$  and  $u$  and not what is going on in each individual lane. This model simplification will ultimately yield a one-dimensional model.

---

<sup>1</sup>Department of Mathematical Sciences, Carnegie Mellon University, Pittsburgh, PA, USA. This research was partially supported by the Applied Mathematical Sciences Program, U. S. Department of Energy and the U. S. National Science Foundation. (greenber@andrew.cmu.edu)

<sup>2</sup>FB Mathematik, TU Darmstadt, Germany. This research was partially supported by the German research foundation (DFG). (klar@mathematik.tu-darmstadt.de)

<sup>3</sup>Laboratoire J.A. Dieudonné, UMR CNRS ° 6621, Université de Nice, Parc Valrose, F-06108, Nice Cedex 02, France. This research was partially supported by the CNRS-NSF. (rascle@math.unice.fr)

On such multilane freeways one often observes distinct stable equilibrium relationships between auto velocity and density. Prototypical situations involve two equilibria

$$v = v_1(\rho) > v = v_2(\rho) \quad , \quad 0 \leq \rho < \rho_{\max} \quad (1.1)$$

where  $v_1(\cdot)$  and  $v_2(\cdot)$  are monotone decreasing and satisfy  $v_1(\rho_{\max}) = v_2(\rho_{\max}) = 0$ . The upper curve is typically stable for densities satisfying  $0 \leq \rho \leq \rho_1$  whereas the lower curve is stable for densities satisfying  $\rho_2 \leq \rho \leq \rho_{\max}$ . Our interest is in the situation where  $0 < \rho_2 \leq \rho_1 < \rho_{\max}$  and  $v_2(\rho_2) \leq v_1(\rho_1)$  (see Figure 1 below).

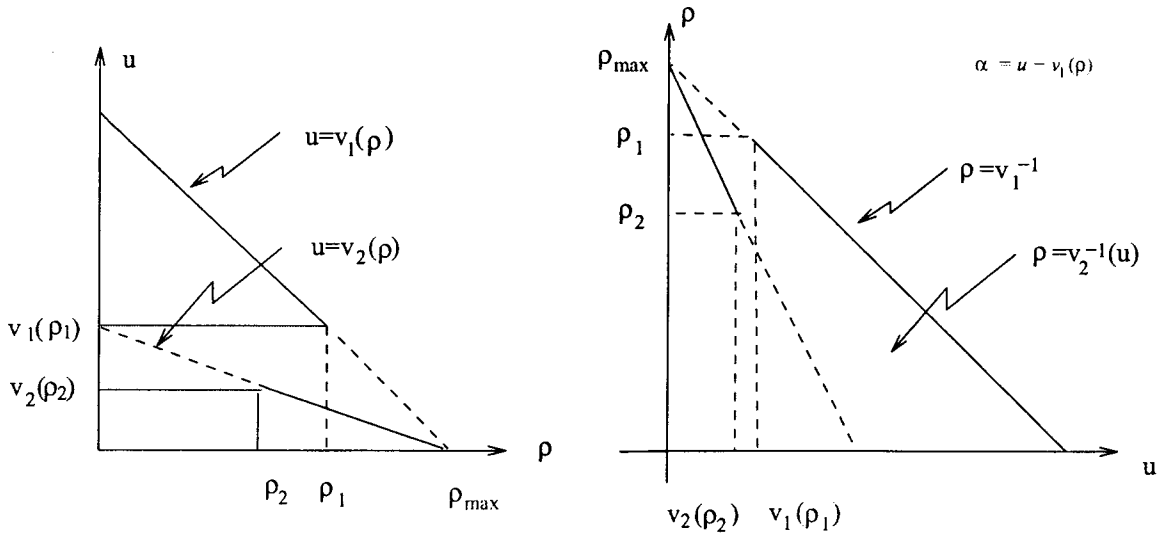


Figure 1

The explanation for the two curves is quite simple. For high density congested traffic lane changing and passing is difficult and dangerous and this yields the slower equilibrium curve. On the other hand, when the traffic is less dense, lane changing and passing becomes easier and this yields the faster equilibrium curve.

In this paper we present a model which incorporates both equilibrium curves and a simple switching mechanism which allows cars to transit from one equilibrium curve to the other.

Once again our basic descriptors are the car density  $\rho$  velocity  $u$ . We also track

$$\alpha = u - v_1(\rho)$$

which represents the discrepancy between the actual car speed and the uncongested equilibrium speed.

Our governing equations are

$$\frac{\partial \rho}{\partial t} + \frac{\partial}{\partial x}(\rho u) = 0 \quad (1.2)$$

and

$$\frac{\partial \alpha}{\partial t} + u \frac{\partial \alpha}{\partial x} = \begin{cases} \frac{-\alpha}{\epsilon} & , \quad \rho < R(u) \\ \frac{((v_2 - v_1)(\rho) - \alpha)}{\epsilon} & , \quad \rho \geq R(u). \end{cases} \quad (1.3)$$

Here,  $u \rightarrow R(u)$  is a monotone non-decreasing function defined on  $0 \leq u$  and satisfying

$$R(u) = \rho_2 \quad , \quad 0 \leq u \leq v_2(\rho_2) \text{ and } R(u) = \rho_1, \quad v_1(\rho_1) \leq u. \quad (1.4)$$

For experimental data and the choice of the switch curve we refer to the work of B. Kerner [7, 8]. In his thesis, Sopasakis [9] gave an argument supporting the choice  $\rho_2 = \rho_1$  and  $R(u) \equiv \rho_2$ ,  $0 \leq u$ .

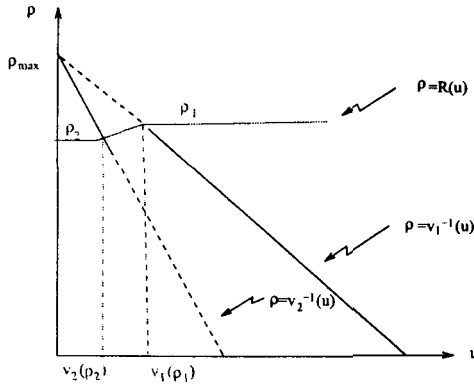


**Figure 2**

The motivation for system (1.2), (1.3) is as follows:

1. When there is no source term, i.e. the right hand side of (1.3) is set to zero, our model is the one introduced in [3]. This model turns out to be the rigorous hydrodynamic limit of the microscopic follow the leader system (1.20)-(1.23) with no right hand side, see [2] and also [10].

2. In the case with a source term of the form  $-1/\epsilon(V(\rho) - u)$  the above result remains true, for details see [6] and [2].

3. At least formally the system we propose to study here is the limit of the microscopic system (1.23), when the size of cars goes to zero.

We note that (1.2) and (1.3) imply that  $u$  satisfies

$$\frac{\partial u}{\partial t} + (u + \rho v_1'(\rho)) \frac{\partial u}{\partial x} = \begin{cases} \frac{v_1(\rho) - u}{\epsilon} & , \quad \rho < R(u) \\ \frac{v_2(\rho) - u}{\epsilon} & , \quad \rho \geq R(u). \end{cases} \quad (1.5)$$

One motivation for the switching mechanism hypothesized here is as follows. We assume there are two natural modes in which drivers can to operate. The first is the fast mode and is characterized



by the equilibrium curve  $\rho \rightarrow v_1(\rho)$  and the second is the slow mode characterized by slow curve  $\rho \rightarrow v_2(\rho)$ . What we are hypothesizing in (1.5) is that if the current state of traffic,  $(u, \rho)$ , lies below the switch curve  $\rho = R(u)$  drivers preferences will migrate towards the fast curve  $u = v_1(\rho)$ , whereas if the traffic state,  $(u, \rho)$ , lies above  $\rho = R(u)$ , their preferences will migrate towards the slow curve  $u = v_2(\rho)$ .

An alternative approach would be to hypothesize that for all densities  $0 \leq \rho \leq \rho_{max}$ , the preferred state of an average driver is characterized by the homogenized equilibrium curve

$$v(\rho) = a(\rho) * v_1(\rho) + (1 - a(\rho)) * v_2(\rho)$$

where  $a(0) = 1$ ,  $a'(\rho) \leq 0$  for  $0 \leq \rho \leq \rho_{max}$ , and  $a(\rho_{max}) = 0$ . This latter approach has been used in multi-class models of traffic flow, see for instance [5], [4] and many other references.

For  $0 < \rho \leq \rho_{max}$ , the system (1.2), (1.4), and (1.5) is strictly hyperbolic with distinct wave speeds  $c_1 = u + \rho v_1'(\rho) < c_2 = u$ . Variants of this relaxation model with one equilibrium and no switch curve have been studied by Aw and Rascle [3], Greenberg et. al [6, 1], and Aw, Klar, Materne, and Rascle [2]. The principal results of those investigations relevant to us here are that for any initial data  $\rho_0(\cdot)$  and  $u_0(\cdot)$  satisfying

$$0 \leq u_0(x) \leq v_1(\rho_0(x)) \text{ and } 0 \leq \rho_0(x) \leq \rho_{max} \quad (1.6)$$

the system (1.2), (1.4) and (1.5) has an appropriately defined weak solution satisfying (1.6) for all future times. Thus the model presented here has no signals propagating faster than the car velocities and yields none of the velocity reversals seen in the Payne-Whitham models. These two observations are the basic strength of this class of second order model.

For simplicity we restrict our attention to spatially periodic solutions – the ring road scenario. We shall also work with a Lagrangian reformulation of the system. When discretized this Lagrangian system yields a follow-the-leader type model.

We let  $l$  be the spatial period of our data  $\rho_0(\cdot) > 0$  and assume that

$$\int_0^l \rho_0(\xi) d\xi = M \quad (1.7)$$

is an integer. For any real number  $m \in [0, M]$  we let  $x^0(m)$  be the unique solution of

$$m = \int_0^{x^0(m)} \rho_0(\xi) d\xi \quad (1.8)$$

and  $x(m, t)$  be the solution of

$$\frac{\partial x}{\partial t}(m, t) = \bar{u}(m, t) \stackrel{\text{def}}{=} u(x(m, t), t) \text{ and } x(m, 0) = x^0(m). \quad (1.9)$$

Here,  $\rho$  and  $u$  are solutions of (1.2), (1.4) and (1.5). The continuity equation (1.2), when combined with (1.8) and (1.9) yields

$$m = \int_{x(0,t)}^{x(m,t)} \rho(\xi, t) d\xi \quad (1.10)$$

and (1.10) in turn implies that

$$\bar{\rho}(m, t) \stackrel{def}{=} \rho(x(m, t), t) \quad \text{and} \quad \bar{\gamma}(m, t) \stackrel{def}{=} \frac{\partial x}{\partial m}(m, t) \quad (1.11)$$

satisfy

$$\bar{\rho}(m, t) \bar{\gamma}(m, t) \equiv 1. \quad (1.12)$$

Additionally (1.9) implies that  $\bar{\gamma}$  and  $\bar{u}$  satisfy

$$\frac{\partial \bar{\gamma}}{\partial t}(m, t) = \frac{\partial \bar{u}}{\partial m}(m, t). \quad (1.13)$$

Finally, if we let

$$\bar{\alpha}(m, t) \stackrel{def}{=} \alpha(x(m, t), t) = \bar{u}(m, t) - V_1(\bar{\gamma}(m, t)), \quad (1.14)$$

then (1.3) implies

$$\frac{\partial \bar{\alpha}}{\partial t}(m, t) = \begin{cases} -\frac{\bar{\alpha}(m, t)}{\epsilon} & , \quad \bar{\gamma}(m, t) > \frac{1}{R(\bar{u}(m, t))} \\ \frac{((V_2 - V_1)(\bar{\gamma}(m, t)) - \bar{\alpha}(m, t))}{\epsilon} & , \quad \bar{\gamma}(m, t) \leq \frac{1}{R(\bar{u}(m, t))} \end{cases} \quad (1.15)$$

where

$$V_1(\bar{\gamma}) \stackrel{def}{=} v_1(1/\bar{\gamma}) \quad \text{and} \quad V_2(\bar{\gamma}) \stackrel{def}{=} v_2(1/\bar{\gamma}). \quad (1.16)$$

In what follows we assume the functions  $V_1(\cdot)$  and  $V_2(\cdot)$  defined in (1.16) are increasing and concave on  $[L \stackrel{def}{=} 1/\rho_{\max}, \infty)$  and satisfy

$$0 = V_2(L^+) = V_1(L^+) \quad \text{and} \quad 0 < V_2^{(p)}(\bar{\gamma}) < V_1^{(p)}(\bar{\gamma}) \quad \text{for} \quad L < \bar{\gamma} < \infty \quad \text{and} \quad p = 0, 1 \quad (1.17)$$

and the limit relations

$$\lim_{\bar{\gamma} \rightarrow \infty} (V_i(\bar{\gamma}), V_i^{(p)}(\bar{\gamma})) = (v_i^\infty, 0), \quad i \quad \text{and} \quad p = 1, 2 \quad (1.18)$$

where  $v_2^\infty < v_1^\infty$ . The parameter  $L$  has the interpretation of the length of a typical car on the roadway.

Equations (1.13) - (1.15) also combine to give

$$\frac{\partial \bar{u}}{\partial t}(m, t) - V_1'(\bar{\gamma}(m, t)) \frac{\partial \bar{u}}{\partial m}(m, t) = \begin{cases} \frac{V_1(\bar{\gamma}(m, t)) - \bar{u}(m, t)}{\epsilon} & , \quad \bar{\gamma}(m, t) > \frac{1}{R(\bar{u}(m, t))} \\ \frac{V_2(\bar{\gamma}(m, t)) - \bar{u}(m, t)}{\epsilon} & , \quad \bar{\gamma}(m, t) \leq \frac{1}{R(\bar{u}(m, t))} \end{cases} \quad (1.19)$$

### The Follow-the-Leader Model

In [6] Greenberg showed that for the Lagrangian system (1.9) - (1.19) the appropriate stable spatial differencing scheme was downwind. Moreover, such differencing, with  $\Delta m = 1$  (recall cars are discrete), yields

$$\frac{dx_m}{dt} = \bar{u}_m, \quad (1.20)$$

$$\bar{\gamma}_m = x_{m+1} - x_m, \quad (1.21)$$

$$\bar{\rho}_m = \frac{1}{\bar{\gamma}_m}, \quad (1.22)$$

and

$$\begin{aligned} & \frac{d\bar{u}_m}{dt} - V_1'(x_{m+1} - x_m)(\bar{u}_{m+1} - \bar{u}_m) \\ &= \begin{cases} \frac{V_1(x_{m+1} - x_m) - \bar{u}_m}{\epsilon}, & x_{m+1} - x_m > \frac{1}{R(\bar{u}_m)} \\ \frac{V_2(x_{m+1} - x_m) - \bar{u}_m}{\epsilon}, & x_{m+1} - x_m \leq \frac{1}{R(\bar{u}_m)}. \end{cases} \end{aligned} \quad (1.23)$$

This latter system implies that

$$\bar{\alpha}_m \stackrel{def}{=} \bar{u}_m - V_1(x_{m+1} - x_m) \quad (1.24)$$

satisfies

$$\frac{d\bar{\alpha}_m}{dt} = \begin{cases} -\frac{\bar{\alpha}_m}{\epsilon}, & x_{m+1} - x_m > \frac{1}{R(\bar{u}_m)} \\ \frac{((V_2 - V_1)(x_{m+1} - x_m) - \bar{\alpha}_m)}{\epsilon}, & x_{m+1} - x_m \leq \frac{1}{R(\bar{u}_m)}. \end{cases} \quad (1.25)$$

These equations hold for  $1 \leq m \leq M$  and  $x_{M+1}(t) = x_1(t) + l$  where again  $l$  is the spatial period of our original data  $\rho_0(\cdot)$  and  $u_0(\cdot)$ . The initial positions of the cars are constrained to satisfy

$$x_{m+1}(0) - x_m(0) \geq L \stackrel{def}{=} \frac{1}{\rho_{\max}} \quad (1.26)$$

and these numbers are related to  $\rho_0(\cdot)$  by

$$\int_{x_m(0)}^{x_{m+1}(0)} \rho_0(\xi) d\xi \stackrel{def}{=} \bar{\rho}_m^0(x_{m+1}(0) - x_m(0)) = 1. \quad (1.27)$$

In section 2 we analyze a first-order integration scheme for the system (1.20) - (1.22), (1.24), and (1.25). We obtain estimates which guarantee that

$$L \leq x_{m+1}(t) - x_m(t) \text{ and } 0 \leq u_m(t) \leq V_1(x_{m+1}(t) - x_m(t)) \quad (1.28)$$

for all  $t \geq 0$ . These estimates guarantee the consistency of the model. In Section 3 we present some simulations with the discrete model. Here we see the persistent periodic wave trains separating congested regions of slow moving traffic from regions of less dense faster moving traffic. The waves separating these regions are analyzed in Section 4. In that section we revert to continuum model (1.9) and (1.11) - (1.19) because it is analytically easier to work with.

## 2 A Priori Estimates

In this section we establish a-priori estimates for solutions of (1.20) - (1.22), (1.24) and (1.25). We integrate these equations with a first-order Euler Scheme. Specifically, we let  $\Delta t$  be our time step,  $t_n = n\Delta t$ , and for any function  $f_m(\cdot)$  we let  $f_m^n$  denote the approximate value of  $f_m(\cdot)$  at  $t_n$ . Our integration scheme is

$$x_m^{n+1} = x_m^n + \Delta t u_m^n, \quad (2.1)$$

$$\bar{\gamma}_m^{n+1} = x_{m+1}^{n+1} - x_m^{n+1}, \quad (2.2)$$

$$\bar{\rho}_m^{n+1} = \frac{1}{(x_{m+1}^{n+1} - x_m^{n+1})}, \quad (2.3)$$

$$\bar{\alpha}_m^{n+1} = (\bar{u}_m^{n+1} - V_1(x_{m+1}^{n+1} - x_m^{n+1})), \quad (2.4)$$

where

$$\bar{\alpha}_m^{n+1} = (1 - \Delta t/\epsilon) \bar{\alpha}_m^n + \Delta t(V_2 - V_1)(x_{m+1}^n - x_m^n)H(\bar{\rho}_m^n - R(\bar{u}_m^n))/\epsilon, \quad (2.5)$$

and

$$H(s) = \begin{cases} 0 & , s < 0 \\ 1 & , s \geq 0. \end{cases} \quad (2.6)$$

These equations hold for  $1 \leq m \leq M$  and

$$x_{M+1}^{n+1} = x_1^{n+1} + l. \quad (2.7)$$

Throughout, we assume that

$$0 \leq \Delta t V_1'(L) \leq 1/2 \text{ and } 0 \leq \Delta t/\epsilon \leq 1/2. \quad (2.8)$$

**Theorem 1** Suppose (2.8) holds and that for  $1 \leq m \leq M$

$$L \leq x_{m+1}^n - x_m^n \quad \text{and} \quad 0 \leq u_m^n \leq V_1(x_{m+1}^n - x_m^n). \quad (2.9)$$

---

<sup>1</sup>Recall, in section 1 we assumed  $\Delta m = 1$  in order to obtain the follow-the-leader model. If, instead we had allowed any  $0 < \Delta m$  our equations (2.2) and (2.3) would have been replaced by  $\tilde{\gamma}_m^{n+1} = (x_{m+1}^{n+1} - x_m^{n+1}) / \Delta m$  and  $\tilde{\rho}_m^{n+1} = \Delta m / (x_{m+1}^{n+1} - x_m^{n+1})$ . Our basic integration scheme (2.1) and (2.5) would be the same but (2.8)<sub>1</sub>, would be modified to  $\frac{\Delta t}{\Delta m} V_1'(L) \leq \frac{1}{2}$ .

Then (2.9) holds for  $n$  replaced by  $n + 1$ . ■

**Proof.** The identities (2.1) - (2.6) imply that

$$\bar{\gamma}_m^{n+1} = \bar{\gamma}_m^n + \Delta t (\bar{u}_{m+1}^n - \bar{u}_m^n) \quad (2.10)$$

and

$$\begin{aligned} \bar{u}_m^{n+1} = & V_1 (\bar{\gamma}_m^{n+1}) + (\bar{u}_m^n - V_1 (\bar{\gamma}_m^n)) (1 - \Delta t/\epsilon) \\ & + (V_2 - V_1) (\bar{\gamma}_m^n) H (\bar{\rho}_m^n - R(\bar{u}_m^n)) \Delta t/\epsilon \end{aligned} \quad (2.11)$$

and the inequalities

$$\left. \begin{aligned} L \leq \bar{\gamma}_m^n \quad , \quad 1 \leq m \leq M \\ 0 \leq \bar{u}_m^n = V_1 (\bar{\gamma}_m^n) + \bar{\alpha}_m^n \quad \text{and} \quad \bar{\alpha}_m^n \leq 0 \quad , \quad 1 \leq m \leq M \end{aligned} \right\} \quad (2.12)$$

imply that

$$\bar{\gamma}_m^{n+1} \geq F (\bar{\gamma}_m^n) \stackrel{def}{=} \bar{\gamma}_m^n - \Delta t V_1 (\bar{\gamma}_m^n). \quad (2.13)$$

The fact that  $\Delta t$  satisfies (2.8) implies that  $F(\cdot)$  is monotone increasing on  $[L, \infty)$  and thus (2.9) and (2.13) imply

$$\bar{\gamma}_m^{n+1} \geq F(L) = L \quad (2.14)$$

as desired. On the other hand the inequalities

$$\bar{u}_m^n - V_1 (\bar{\gamma}_m^n) \leq 0 \quad \text{and} \quad (V_2 - V_1) (\bar{\gamma}_m^n) \leq 0 \quad (2.15)$$

and (2.11) imply that

$$\bar{\alpha}_m^{n+1} = \bar{u}_m^{n+1} - V_1 (\bar{\gamma}_m^{n+1}) \leq 0. \quad (2.16)$$

The identity (2.11) when combined with (2.10) yields

$$\begin{aligned} \bar{u}_m^{n+1} = & (1 - \Delta t/\epsilon) \bar{u}_m^n + (V_1 (\bar{\gamma}_m^n + \Delta t (\bar{u}_{m+1}^n - \bar{u}_m^n)) - V_1 (\bar{\gamma}_m^n)) \\ & + (\Delta t/\epsilon) (1 - H (\bar{\rho}_m^n - R(\bar{u}_m^n))) V_1 (\bar{\gamma}_m^n) \\ & + (\Delta t/\epsilon) H (\bar{\rho}_m^n - R(\bar{u}_m^n)) V_2 (\bar{\gamma}_m^n) \end{aligned} \quad (2.17)$$

or

$$\begin{aligned} \bar{u}_m^{n+1} = & (1 - \Delta t/\epsilon - \Delta t V_1'(\delta_m^n)) \bar{u}_m^n + \Delta t V_1'(\delta_m^n) \bar{u}_{m+1}^n \\ & + (\Delta t/\epsilon) (1 - H (\bar{\rho}_m^n - R(\bar{u}_m^n))) V_1 (\bar{\gamma}_m^n) + (\Delta t/\epsilon) H (\bar{\rho}_m^n - R(\bar{u}_m^n)) V_2 (\bar{\gamma}_m^n), \end{aligned} \quad (2.18)$$

for some  $\delta_m^n \geq \min(\gamma_m^{n+1}, \gamma_m^n) \geq L$  and (2.18) together with (2.6) and (2.8) and  $u_m^n \geq 0$ ,  $1 \leq m \leq M$ , implies that  $\bar{u}_m^{n+1} \geq 0$ . This concludes the proof of Theorem 1. ■

The estimates contained in Theorem 1 guarantee that the densities

$$\rho_m^n \stackrel{\text{def}}{=} \frac{1}{x_{m+1}^n - x_m^n}, \quad 1 \leq m \leq M \quad (2.19)$$

satisfy

$$0 \leq \rho_m^n \leq \rho_{\max}. \quad (2.20)$$

These estimates further imply that the approximate solutions defined in (2.1) - (2.7) converge to solutions of the follow-the-leader model (1.20) - (1.22), (1.24), and (1.25) as  $\Delta t \rightarrow 0^+$ . This concludes Section 2.

### 3 Simulations

All computations in this section were run with the following equilibrium relations:

$$v_1(\rho) = v_1^\infty(1 - \rho/\rho_{\max}) \text{ and } v_2(\rho) = v_2^\infty(1 - \rho/\rho_{\max}). \quad (3.1)$$

These transform to

$$V_1(\gamma) = v_1^\infty \left(1 - \frac{L}{\gamma}\right) \text{ and } V_2(\gamma) = v_2^\infty \left(1 - \frac{L}{\gamma}\right) \quad (3.2)$$

where  $L = \frac{1}{\rho_{\max}}$ . The specific parameter used were

$$v_1^\infty = 100 \text{ feet/sec} = \frac{100 \times 3600}{5280} = 68.1818\dots \text{ mph} \quad (3.3)$$

$$v_2^\infty = 40 \text{ feet/sec} = \frac{40 \times 3600}{5280} = 27.2727\dots \text{ mph} \quad (3.4)$$

and

$$L = 15 \text{ feet}. \quad (3.5)$$

The latter number corresponds to a maximum car density of

$$\rho_{\max} = \frac{1}{15} \text{ cars/foot} = \frac{5280}{15} = 352 \text{ cars/mile}. \quad (3.6)$$

We used the constant switch curve introduced by Sopasakis [9]:

$$\gamma(u) = \gamma_* \quad , \quad 0 \leq u \quad (3.7)$$

with  $\gamma_* = 20$  feet. For initial data we chose 3 sets of data:

$$x_m^{(k)}(0) = 20m + .1 \sin\left(\frac{km\pi}{200}\right) \quad (3.8)$$

for  $-\infty \leq m \leq \infty$  and  $k = 1, 2$ , and  $3$ . The observation that

$$x_{400}^{(k)}(0) = 8000 \text{ feet} = 1.5151\dots \text{ miles} \quad (3.9)$$

and

$$x_{m+400}^{(k)}(0) = x_m^{(k)}(0) + 8000 \quad (3.10)$$

implies we may interpret the data as initial data for a ring-road with 400 cars which is of length 1.5151... miles. We chose constant initial velocities

$$u_m^{(k)}(0) = .5(V_1(\gamma_*) + V_2(\gamma_*)), \quad 1 \leq m \leq 400 \quad (3.11)$$

or

$$u_m^{(k)}(0) = 17.5 \text{ feet/sec} = 11.931818\dots \text{ mph}, \quad 1 \leq m \leq 400. \quad (3.12)$$

These data guarantee points on both sides of the switch curve. Simulations were run with relaxation times

$$\epsilon = 1, 2, 4, \text{ and } 8. \quad (3.13)$$

Below, we show the long-time spatially and temporally periodic solutions at time  $t = 2$  hours when  $\epsilon = 8$  seconds. Figures 3, 4, and 5 correspond to the initial data indexed by  $k = 1, 2$ , and  $3$  respectively. At earlier times the solution indexed by each particular  $k$  had  $k$  discontinuities per period. This phenomena persisted to  $t = 2$  hours for the solution indexed by  $k = 2$  but the solution corresponding to the index  $k = 3$  converged, by  $t = 2$  hours, to a solution with one discontinuity per period.

The first two frames in each figure are self-explanatory. In the third frame of each figure we plot the curve  $m \rightarrow (\gamma_m = x_{m+1} - x_m, u_m)$ . This curve is shown in black. The blue curves are the equilibrium curves  $\gamma \rightarrow (\gamma, V_1(\gamma))$  and  $\gamma \rightarrow (\gamma, V_2(\gamma))$  and the red curve is the image of  $u \rightarrow (20, u)$ . The red dot - o - is the image of  $(\gamma_1, u_1)$ . Complete animations of all of these simulations may be found at [//www.math.cmu.edu/~plin/congestion/](http://www.math.cmu.edu/~plin/congestion/). The discontinuities in the profiles propagate at the speed

$$c \simeq 227.6 \pm .1 \text{ cars/minute.} \quad (3.14)$$

An analysis of these solutions may be found in Section 4.



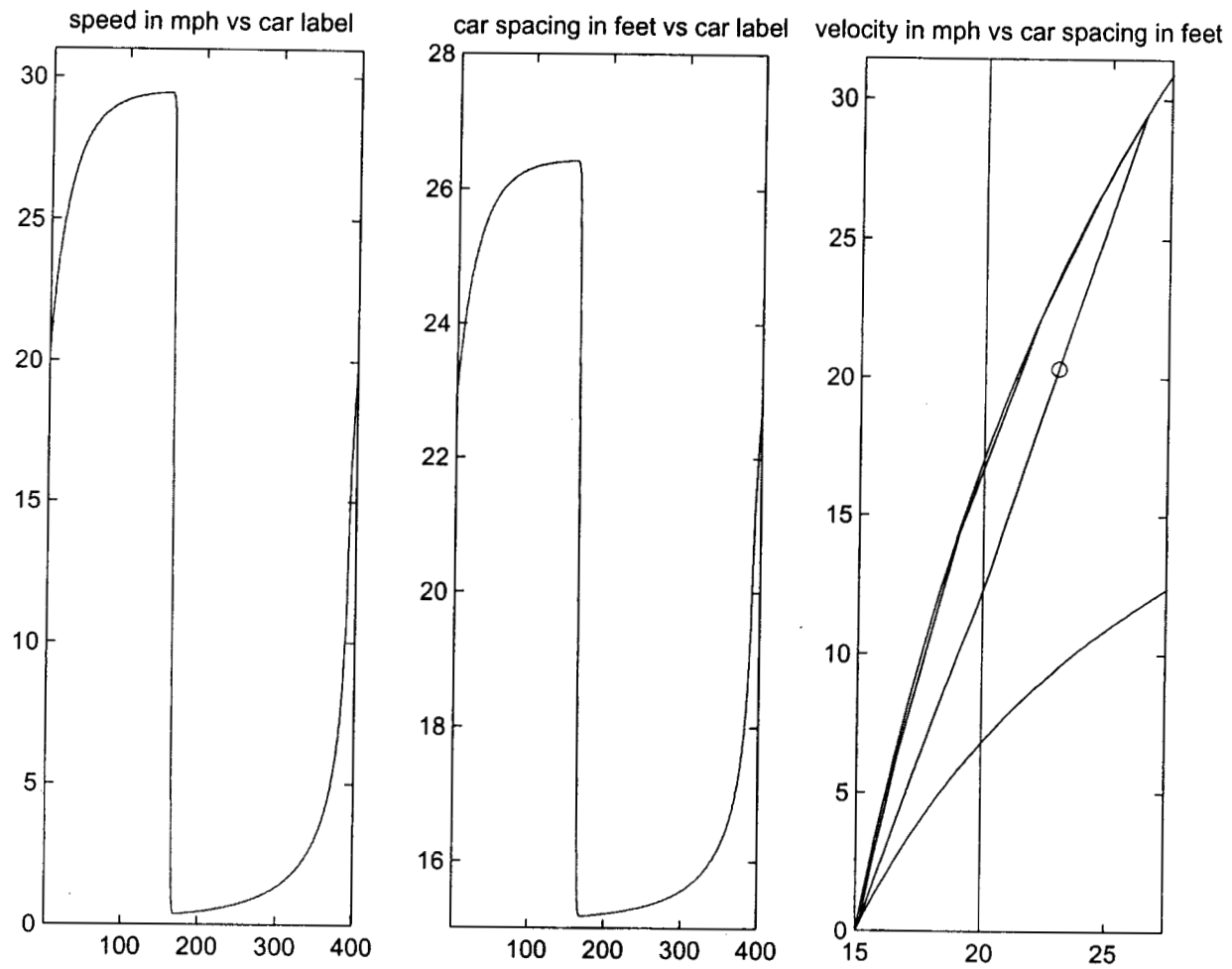
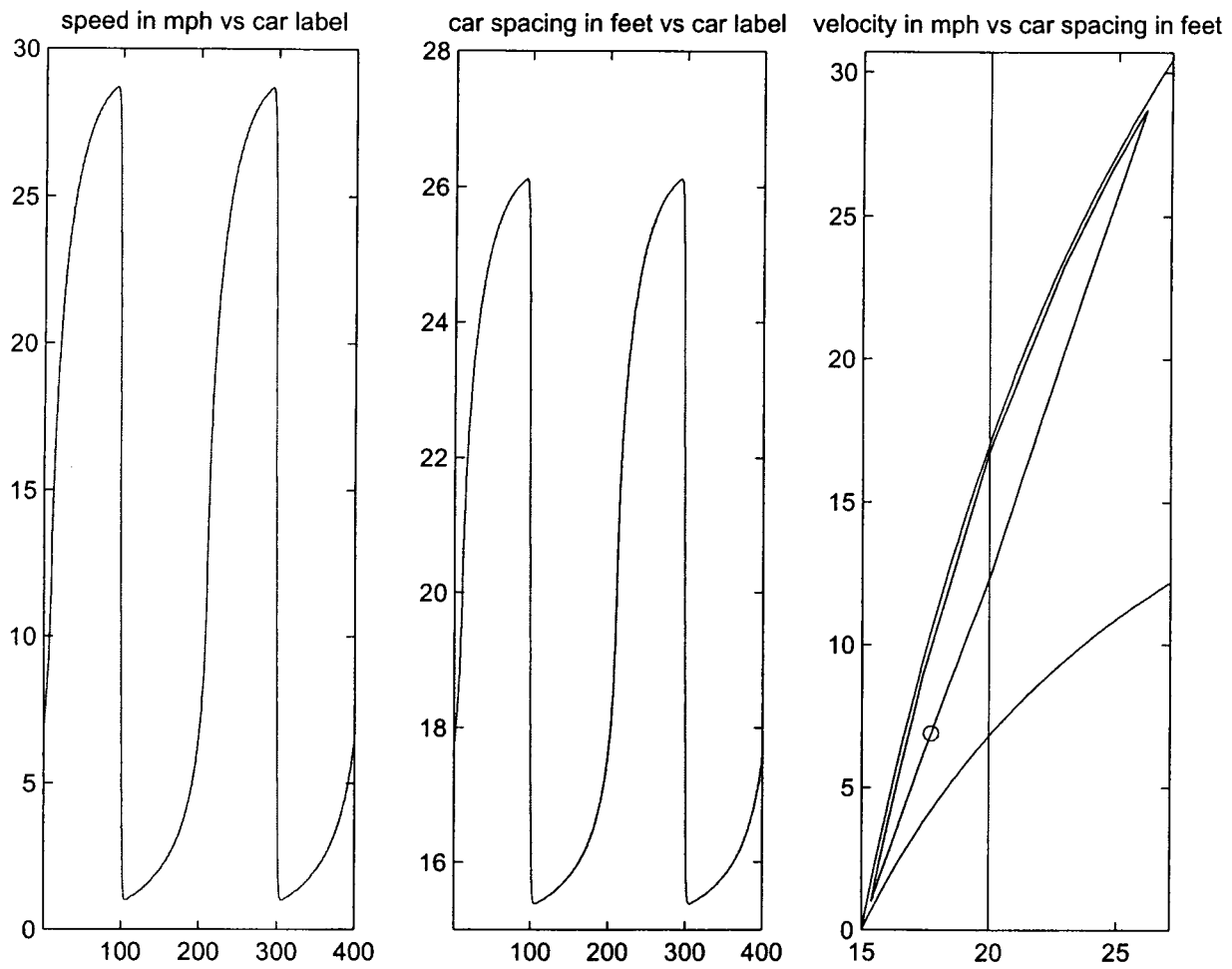


Figure 3



**Figure 4**

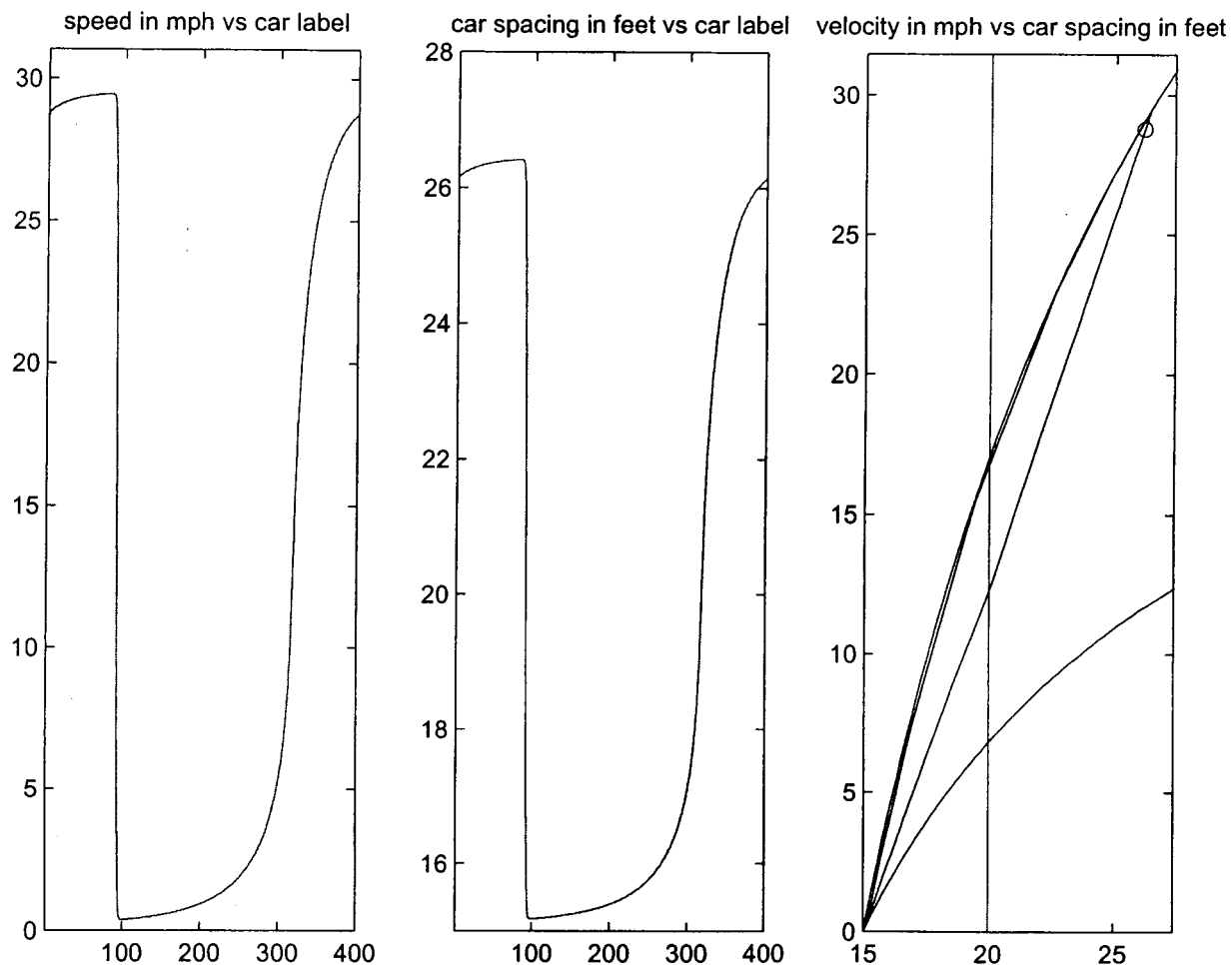


Figure 5

## 4 Travelling Waves

The wave trains obtained in section 3 are basically discrete approximations to travelling wave solutions to the continuum equations (1.9) - (1.19). In this section our goal is to show that the continuum system (1.9) - (1.19) actually supports such travelling waves. For definiteness we shall assume that the switch curve introduced in (1.4) is the one derived by Sopasakis in [9], namely the curve

$$R(u) = \rho_* \quad , \quad 0 \leq u. \quad (4.1)$$

With this choice of switch curve the Lagrangian equations become

$$\frac{\partial \bar{\gamma}}{\partial t} - \frac{\partial \bar{u}}{\partial m} = 0 \text{ and } \frac{\partial \bar{u}}{\partial t} - V_1'(\bar{\gamma}) \frac{\partial \bar{u}}{\partial m} = \begin{cases} \frac{V_1(\bar{\gamma}) - \bar{u}}{\epsilon}, & \bar{\gamma} > \gamma_* = \frac{1}{\rho_*} \\ \frac{V_2(\bar{\gamma}) - \bar{u}}{\epsilon}, & \bar{\gamma} \leq \gamma_* = \frac{1}{\rho_*}. \end{cases} \quad (4.2)$$

Once again

$$V_1(\bar{\gamma}) = v_1(1/\bar{\gamma}) \text{ and } V_2(\bar{\gamma}) = v_2(1/\bar{\gamma}) \quad (4.3)$$

and we assume that both  $V_1$  and  $V_2$  are increasing and concave on  $[L, \infty)$  and satisfy

$$0 = V_2(L^+) = V_1(L^+) \text{ and } 0 < V_2^{(p)}(\bar{\gamma}) < V_1^{(p)}(\bar{\gamma}) \text{ for } L < \bar{\gamma} < \infty \text{ and } p = 0, 1 \quad (4.4)$$

and the limit relations

$$\lim_{\bar{\gamma} \rightarrow \infty} (V_i(\bar{\gamma}), V_i^{(p)}(\bar{\gamma})) = (v_i^\infty, 0), \quad i \text{ and } p = 1, 2 \quad (4.5)$$

where  $0 < v_2^\infty < v_1^\infty$ .  $L$  is related to  $\rho_{\max}$  by  $L = 1/\rho_{\max}$ .

We start by describing the portion of the wave trains where both  $\bar{\gamma}$  and  $\bar{u}$  are increasing in  $m$ . These solutions are functions of

$$\xi = m + ct \quad (4.6)$$

and are normalized so that

$$\bar{\gamma}(0) = \gamma_* \text{ and } V_2(\gamma_*) < u_* < V_1(\gamma_*). \quad (4.7)$$

Once again  $\gamma_* = \frac{1}{\rho_*}$  (see (4.1)). Equation (4.2)<sub>1</sub>, implies that  $\bar{u} = u_* + c(\bar{\gamma} - \gamma_*)$  while (4.2)<sub>2</sub> yields

$$c(c - V_1'(\bar{\gamma})) \frac{d\bar{\gamma}}{d\xi} = \begin{cases} \frac{V_1(\bar{\gamma}) - u_* - c(\bar{\gamma} - \gamma_*)}{\epsilon}, & \bar{\gamma} > \gamma_* \\ \frac{V_2(\bar{\gamma}) - u_* - c(\bar{\gamma} - \gamma_*)}{\epsilon}, & \bar{\gamma} \leq \gamma_*. \end{cases} \quad (4.8)$$

The requirement that  $\bar{\gamma}$  is increasing in  $\xi$  implies that  $\bar{\gamma}$  must satisfy  $\frac{d\bar{\gamma}}{d\xi}(0^-) \geq 0$  and  $\frac{d\bar{\gamma}}{d\xi}(0^+) \geq 0$ .

Equations (4.7) and (4.8) then imply that these latter inequalities may only be met if

$$c = V_1'(\gamma_*). \quad (4.9)$$

In what follows we let  $\Gamma_* > L$  be the unique solution of

$$V_1'(\Gamma_*) = V_2'(L^+). \quad (4.10)$$

If  $L < \gamma_* < \Gamma_*$ , we let

$$\bar{U} = V_1'(\gamma_*)(\gamma_* - L) \quad (4.11)$$

and note that for  $V_2(\gamma_*) < u_* < \bar{U}$  the equation

$$u_* + V_1'(\gamma_*)(\bar{\gamma} - \gamma_*) = V_2(\bar{\gamma}) \quad (4.12)$$

has a unique solution  $\gamma_- \in (L, \gamma_*)$  satisfying

$$V_1'(\gamma_*) > V_2'(\gamma_-). \quad (4.13)$$

On the other hand, if  $\Gamma_* < \gamma_*$  we let  $\gamma_l \in (L, \gamma_*)$  be the unique solution of

$$V_2'(\gamma_l) = V_1'(\gamma_*) \quad (4.14)$$

and

$$\bar{U} = V_1'(\gamma_*)(\gamma_* - \gamma_l) + V_2(\gamma_l) \quad (4.15)$$

and note that for  $V_2(\gamma_*) < u_* < \bar{U}$  the equation (4.11) has a unique solution  $\gamma_- \in (\gamma_l, \gamma_*)$  satisfying (4.12).

In what follows we assume the parameter  $u_*$  in (4.8) satisfies  $V_2(\gamma_*) < u_* \leq \bar{U}$  where  $\bar{U}$  is defined in (4.10) or (4.14) as appropriate.

We now note that (4.2)<sub>2</sub>, when combined with (4.8), implies that the profile  $\bar{\gamma}$  must satisfy

$$V_1'(\gamma_*) (V_1'(\gamma_*) - V_1'(\bar{\gamma})) \frac{d\bar{\gamma}}{d\xi} = \begin{cases} \frac{V_1(\bar{\gamma}) - u_* - V_1'(\gamma_*)(\bar{\gamma} - \gamma_*)}{\epsilon}, & \bar{\gamma} > \gamma_* \\ \frac{V_2(\bar{\gamma}) - u_* - V_1'(\gamma_*)(\bar{\gamma} - \gamma_*)}{\epsilon}, & \bar{\gamma} \leq \gamma_* \end{cases} \quad (4.16)$$

Once again, we normalize the profile by insisting that (4.7) holds

Noting that  $\text{sign}(V_1'(\gamma_*) - V_1'(\bar{\gamma})) = \text{sign}(\bar{\gamma} - \gamma_*)$ , that

$$V_1(\bar{\gamma}) - u_* - V_1'(\gamma_*)(\bar{\gamma} - \gamma_*) > 0 \quad , \quad \gamma_* < \bar{\gamma} < \gamma_+ \quad (4.17)$$

where  $\gamma_* < \gamma_+$  is the unique solution of

$$V_1(\gamma_+) - u_* - V_1'(\gamma_*)(\gamma_+ - \gamma_*) = 0, \quad (4.18)$$

and finally that

$$V_2(\bar{\gamma}) - u_* - V_1'(\gamma_*)(\bar{\gamma} - \gamma_*) < 0 \quad , \quad \gamma_- < \bar{\gamma} < \gamma_* \quad (4.19)$$

where  $\gamma_-$  is defined in (4.11) we see that (4.15) and (4.16) has a unique increasing solution defined on  $(-\infty, \infty)$ . For  $\xi < 0$  the solution is given by the quadrature formula

$$\epsilon V_1'(\gamma_*) \int_{\bar{\gamma}(\xi)}^{\gamma_*} \frac{(V_1'(\eta) - V_1'(\gamma_*))d\eta}{(u_* + V_1'(\gamma_*)(\eta - \gamma_*) - V_2(\eta))} = -\xi \quad (4.20)$$

and for  $\xi > 0$  the solution is given by

$$\epsilon V_1'(\gamma_*) \int_{\gamma_*}^{\bar{\gamma}(\xi)} \frac{(V_1'(\gamma_*) - V_1'(\eta))d\eta}{(V_1(\eta) - u_* - V_1'(\gamma_*)(\eta - \gamma_*))} = \xi. \quad (4.21)$$

### Periodic Profiles

For any  $\bar{\gamma} \in (\gamma_-, \gamma_*)$ , we let  $\Gamma(\bar{\gamma}) > \gamma_*$  be the unique solution of

$$V_1(\Gamma(\bar{\gamma})) - V_1(\bar{\gamma}) = V_1'(\gamma_*)(\Gamma(\bar{\gamma}) - \bar{\gamma}) \quad (4.22)$$

and note that

$$\frac{d\Gamma(\bar{\gamma})}{d\bar{\gamma}} = \frac{(V_1'(\bar{\gamma}) - V_1'(\gamma_*))}{(V_1'(\Gamma(\bar{\gamma})) - V_1'(\gamma_*))} < 0. \quad (4.23)$$

We are now in a position to define the periodic wave trains. For  $-|\xi_a| < \xi \leq 0$ ,  $\bar{\gamma}(\xi)$  is given by (4.20) and  $|\xi_a|$  is given by

$$\epsilon V_1'(\gamma_*) \int_{\bar{\gamma}_a}^{\gamma_*} \frac{(V_1'(\eta) - V_1'(\gamma_*))d\eta}{(u_* + V_1'(\gamma_*)(\eta - \gamma_*) - V_2(\eta))} \stackrel{def}{=} |\xi_a| \quad (4.24)$$

where  $\gamma_- < \bar{\gamma}_a < \gamma_*$ . For  $0 \leq \xi \leq \xi_{\Gamma(\bar{\gamma}_a)}$ ,  $\bar{\gamma}(\xi)$  is given by (4.21) and  $\xi_{\Gamma(\bar{\gamma}_a)}$  is given by

$$\epsilon V_1'(\gamma_*) \int_{\gamma_*}^{\Gamma(\bar{\gamma}_a)} \frac{(V_1'(\gamma_*) - V_1'(\eta))d\eta}{(V_1(\eta) - u_* - V_1'(\gamma_*)(\eta - \gamma_*))} \stackrel{def}{=} \xi_{\Gamma(\bar{\gamma}_a)}. \quad (4.25)$$

We extend these solutions to all  $\xi$  via

$$\bar{\gamma}(\xi) = \bar{\gamma}(\xi + \xi_{\Gamma(\bar{\gamma}_a)} + |\xi_a|). \quad (4.26)$$

The extended solution is a proper weak solution to (4.2). The relations (4.9) and (4.22) imply that the Rankine-Hugoniot relations for (4.2) hold across the discontinuities

$$\xi = m + V_1'(\gamma_*)t = \xi_{\Gamma(\bar{\gamma}_a)} \pm n (\xi_{\Gamma(\bar{\gamma}_a)} + |\xi_a|), n = 0, 1, \dots \quad (4.27)$$

(4.22) also implies that

$$V_1'(\bar{\gamma}_a) > V_1'(\gamma_*) = \frac{V_1(\Gamma(\bar{\gamma}_a)) - V_1(\bar{\gamma}_a)}{\Gamma(\bar{\gamma}_a) - \bar{\gamma}_a} > V_1'(\Gamma(\bar{\gamma}_a)) \quad (4.28)$$

and thus across these discontinuities the Lax entropy condition is satisfied. Recalling that the particular solutions of interest to us must be  $M$  periodic, we see that (4.24) and (4.25) imply that for some integer  $k \geq 1$ ,  $\bar{\gamma}_a$  and  $u_*$  must be such that

$$k \in V_1'(\gamma_*) \left[ \int_{\bar{\gamma}_a}^{\gamma_*} \frac{(V_1'(\eta) - V_1'(\gamma_*))d\eta}{(u_* + V_1'(\gamma_*)(\eta - \gamma_*) - V_2(\eta))} + \int_{\gamma_*}^{\Gamma(\bar{\gamma}_a)} \frac{(V_1'(\gamma_*) - V_1'(\eta))d\eta}{(V_1(\eta) - u_* - V_1'(\gamma_*)(\eta - \gamma_*))} \right] = M. \quad (4.29)$$

The condition that  $x(M, t) = x(1, t) + l$  implies that  $\bar{\gamma}_a$  and  $u_*$  must also satisfy

$$k \in V_1'(\gamma_*) \left[ \int_{\bar{\gamma}_a}^{\gamma_*} \frac{(V_1'(\eta) - V_1'(\gamma_*))\eta d\eta}{(u_* + V_1'(\gamma_*)(\eta - \gamma_*) - V_2(\eta))} + \int_{\gamma_*}^{\Gamma(\bar{\gamma}_a)} \frac{(V_1'(\gamma_*) - V_1'(\eta))\eta d\eta}{(V_1(\eta) - u_* - V_1'(\gamma_*)(\eta - \gamma_*))} \right] = l. \quad (4.30)$$

We conclude this section with an analysis of the equations (4.29) and (4.30). We first note that the integer  $k \geq 1$  in these equations is equal to the number of discontinuities of  $\bar{\gamma}(\cdot)$  per period. We also note that instead of using  $u_*$  and  $\bar{\gamma}_a$  as our basic parameters we may instead use  $\gamma_-$  and  $\bar{\gamma}_a$ . With this choice

$$u_* + V_1'(\gamma_*)(\eta - \gamma_*) - V_2(\eta) = V_2(\gamma_-) + V_1'(\gamma_*)(\eta - \gamma_-) - V_2(\eta) > 0, \gamma_- < \eta < \gamma_* \quad (4.31)$$

and

$$V_1(\eta) - u_* - V_1'(\gamma_*)(\eta - \gamma_*) = V_1(\eta) - V_2(\gamma_-) - V_1'(\gamma_*)(\eta - \gamma_-) > 0, \gamma_* < \eta < \Gamma(\gamma_-) \quad (4.32)$$

and solving (4.29) and (4.30) is equivalent to finding  $\bar{\gamma}_a \in (\gamma_-, \gamma_*)$  and  $\gamma_- < \gamma_*$  such that

$$k \in V_1'(\gamma_*) \left[ \int_{\bar{\gamma}_a}^{\gamma_*} \frac{(V_1'(\eta) - V_1'(\gamma_*))d\eta}{(V_2(\gamma_-) + V_1'(\gamma_*)(\eta - \gamma_-) - V_2(\eta))} + \int_{\gamma_*}^{\Gamma(\bar{\gamma}_a)} \frac{(V_1'(\gamma_*) - V_1'(\eta))d\eta}{(V_1(\eta) - V_2(\gamma_-) - V_1'(\gamma_*)(\eta - \gamma_-))} \right] = M \quad (4.33)$$

and

$$k \in V_1'(\gamma_*) \left[ \int_{\bar{\gamma}_a}^{\gamma_*} \frac{(V_1'(\eta) - V_1'(\gamma_*))\eta d\eta}{(V_2(\gamma_-) + V_1'(\gamma_*)(\eta - \gamma_-) - V_2(\eta))} + \int_{\gamma_*}^{\Gamma(\bar{\gamma}_a)} \frac{(V_1'(\gamma_*) - V_1'(\eta))\eta d\eta}{(V_1(\eta) - V_2(\gamma_-) - V_1'(\gamma_*)(\eta - \gamma_-))} \right] = l. \quad (4.34)$$

In what follows we let  $L_1(\gamma_-, \bar{\gamma}_a, \gamma_*)$  and  $L_2(\gamma_-, \bar{\gamma}_a, \gamma_*)$  be the functions defined by the left hand sides of (4.33) and (4.34) respectively. If  $L < \gamma_* < \Gamma_*$  (see (4.9)) the functions  $L_1$  and  $L_2$  are well defined for  $\gamma_- \in (L, \gamma_*)$  and  $\bar{\gamma}_a \in (\gamma_-, \gamma_*)$  whereas if  $\Gamma_* \leq \gamma_*$  these functions are well defined for  $\gamma_- \in (\gamma_l, \gamma_*)$  (see (4.13)) and  $\bar{\gamma}_a \in (\gamma_-, \gamma_*)$ . In either case, the observation that  $\lim_{\bar{\gamma}_a \rightarrow \gamma_*^-} \Gamma(\bar{\gamma}_a) = \gamma_*$  implies that  $L_1(\gamma_-, \gamma_*^-, \gamma_*) = L_2(\gamma_-, \gamma_*^-, \gamma_*) = 0$ . We further note that for  $\gamma_- < \bar{\gamma}_a < \gamma_*$

$$\frac{\partial L_1}{\partial \bar{\gamma}_a}(\gamma_-, \bar{\gamma}_a, \gamma_*) = k \in V_1'(\gamma_*) \left[ \frac{(V_1'(\gamma_*) - V_1'(\bar{\gamma}_a))}{(V_2(\gamma_-) + V_1'(\gamma_*)(\bar{\gamma}_a - \gamma_*) - V_2(\bar{\gamma}_a))} + \frac{d\Gamma(\bar{\gamma}_a)}{d\bar{\gamma}_a} \frac{(V_1'(\gamma_*) - V_1'(\Gamma(\bar{\gamma}_a)))}{(V_1(\Gamma(\bar{\gamma}_a)) - V_2(\gamma_-) - V_1'(\gamma_*)(\Gamma(\bar{\gamma}_a) - \gamma_-))} \right] \quad (4.35)$$

The last identity, together with  $\frac{d\Gamma}{d\bar{\gamma}_a}(\bar{\gamma}_a) < 0$ , implies that  $\frac{\partial L_1}{\partial \bar{\gamma}_a}(\gamma_-, \bar{\gamma}_a, \gamma_*) < 0$ . The fact that

$$\lim_{\bar{\gamma}_a \rightarrow \gamma_-^+} L_1(\gamma_-, \bar{\gamma}_a, \gamma_*) = +\infty \quad (4.36)$$

then guarantees that for each  $L < \gamma_*$  and admissible  $\gamma_-$  there is a unique  $\bar{\gamma}_a(\gamma_-, \gamma_*, M)$  such that (4.33) holds. Thus, solving (4.33) and (4.34) is equivalent to finding an admissible  $\gamma_- < \gamma_*$  so that

$$L_2(\gamma_-, \bar{\gamma}_a(\gamma_-, \gamma_*, M), \gamma_*) = l. \quad (4.37)$$

The integral mean-value theorem, when combined with the definition of  $\bar{\gamma}_a(\gamma_-, \gamma_*, M)$ , guarantees that

$$M\bar{\gamma}_a(\gamma_-, \gamma_*, M) \leq L_2(\gamma_-, \bar{\gamma}_a(\gamma_-, \gamma_*, M), \gamma_*) = Mg \quad (4.38)$$

for some  $g \in (\bar{\gamma}_a(\gamma_-, \gamma_*, M), \Gamma(\bar{\gamma}_a(\gamma_-, \gamma_*, M)))$ . These observations, together with  $\gamma_- < \bar{\gamma}_a(\gamma_-, \gamma_*, M)$  and  $\Gamma(\bar{\gamma}_a(\gamma_-, \gamma_*, M)) < \Gamma(\gamma_-)$ , imply that (4.37) has no solutions for

$$l < \begin{cases} ML, & \text{if } \gamma_* < \Gamma_* \text{ (see (4.9) and (4.22))} \\ M\gamma_l, & \text{if } \gamma_* \geq \Gamma_* \text{ (see (4.9), (4.13), and (4.22))} \end{cases} \quad (4.39)$$

and

$$l > \begin{cases} M\Gamma(L), & \text{if } \gamma_* < \Gamma_* \text{ (see (4.9) and 4.22)} \\ M\Gamma(\gamma_l), & \text{if } \gamma_* \geq \Gamma_* \text{ (see (4.9), (4.13), and (4.22)).} \end{cases} \quad (4.40)$$

These estimates on the range of  $\gamma_- \rightarrow L_2(\gamma_-, \bar{\gamma}_a(\gamma_-, \gamma_*, M), \gamma_*)$ , though not particularly sharp, are all we could manage with this degree of generality on the functions  $V_1(\cdot)$  and  $V_2(\cdot)$ .

## References

- [1] Argall, B., Cheleskin, E., Greenberg, J. M., Hinde, C., and Lin, P. J., A Rigorous Treatment of a Follow-the-Leader Traffic Model with Traffic Lights Present, *SIAM J. Appl. Math.* (submitted).
- [2] Aw, A., Klar, A., Materne, T., and Rascle, M., Derivation of Continuum Traffic Flow Models from Microscopic Follow-the-Leader Models, *to appear in SIAM J. Appl. Math.*



- [3] Aw, A. and Rascle, M., Resurrection of Second Order Models of Traffic Flow? *SIAM J. Appl. Math.*, 60, 3, 916-938, (2000).
- [4] Bagnerini, Rascle, M., A multi-class homogenized hyperbolic model of traffic flow, preprint
- [5] Daganzo, C.F., A behavioral theory of multi-lane traffic flow. Part I: Long homogeneous freeway sections, preprint
- [6] Greenberg, J. M., Extensions and Amplifications of a Traffic Model of Aw and Rascle, *SIAM J. Appl. Math.*, 62,3, 729-745, 2001 .
- [7] Kerner, B.S., Experimental features of self-organization in traffic flow, *Physical Review Letters*, 81, 3797, (1998).
- [8] Kerner, B.S., Congested Traffic Flow, *Transp. Res. Rec.*, 1678, 160, (1998).
- [9] Sopasakis, A., "Unstable Flow and Modeling," *Mathematical and Computer Modeling* (to appear).
- [10] Zhang, M., A nonequilibrium traffic model devoid of gas like behaviour, *Transp. Res. B* , (to appear)